Exact solutions for coupled Duffing oscillators

Exact solutions for coupled Duffing oscillators

Stefano Lenci

Department of Civil and Building Engineering, and Architecture,
Polytechnic University of Marche, 60131 Ancona, Italy

E-mail: lenci@univpm.it

Abstract

The exact analytical solution of a system made of two coupled Duffing oscillators is obtained. The mathematical solution is illustrated by means of some examples aimed at showing the dynamical phenomena occurring in the considered system. Frequency response curves are reported for different value of the parameters, highlighting the effects of the linear and nonlinear coupling between the two variables. The presence of various solution branches, up to four coexisting attractors, is reported.

Keywords. Coupled Duffing oscillators, exact solution, nonlinear resonance, linear and nonlinear coupling.

1 Introduction

Exact mathematical solutions of nonlinear problems are very helpful to perform comprehensive analyses, and to capture the main nonlinear phenomena (subharmonic and superharmonic resonances, nonlinear resonance, bifurcations, chaos, etc.) that characterize these systems with respect to the linear one, that are much simpler, at least in terms of possible outcome. In fact, numerical solutions, while can be useful for investigating a specific case, are not helpful for a detailed parametric analysis aimed at understanding the "whole" system behaviour, that is need, for example, in the pre-design of any mechanical tool or civil structure. Approximate analytical solutions, on the other hand, while helpful because providing general - and often simple [1] - formulas, may miss some phenomena because of their intrinsic approximate nature.

The exact solution of nonlinear problems exist only in few case [2], especially if one considers the dynamical behaviour and do no limit to the statical one. Thus, any new solution is welcome and enlarge the overall knowledge and possibility of application.

Considering deterministic forcing (i.e. not addressing stochastic excitations), in the very large majority of mechanical problems the excitation (external or parametric) is assumed to be not only periodic, but also harmonic (sinusoidal) in time. This is the legacy of the linear realm, in which harmonic excitations are important since they commonly lead to simple and exact solutions. In nonlinear regime this is not the case, and harmonic functions no longer play a relevant role; for example, apart from pathological cases, they do not provide exact solution. In fact, only in few cases the harmonicity of the excitation is really suggested by the application at hand.

They were Harvey [3] and Hsu [4] to realize that relaxing the assumption on harmonicity, but still keeping the periodicity of the excitation, may lead to elegant and relatively simple exact analytical solutions for nonlinear problems. The Hsu statement "...we shall try to find out what type of external forcing function will excite a steady state response, which is an exact solution of the equation of motion, and which is expressible in a simple form" [4] is very illuminating, and opened the way to various further researches.

Hsu [4] considered the Duffing equation [5], and used the elliptic functions [6] of the undamped unforced case to obtain the exact solution in the forced case, assuming that the force is proportional to (i) the linear term, and (ii) to the linear and nonlinear terms, and then generalizing it to multi-term elliptic response. The work of Hsu has been extended to the case of purely nonlinear and to a quadratic oscillators in [7], which reports a very detailed analysis. Still the undamped case is considered, while the damping has been treated in [8] within the same conceptual approach. The inverse problem of designing the excitation to have a desired response, which generalize the ideas of Hsu in choosing the desired outcome, was proposed in [9].

Caughey and Vakakis [10] applied the same ideas of "transforming the forced problem to a free vibration by suitably choosing the form of the excitation" to a two degrees of freedom (dof) nonlinear system. They considered the symmetric case (i.e. both oscillators have the same nonlinear stiffness) and focus on similar nonlinear normal modes, i.e. those for which $y(t) = c\,x(t)$, ($x(t)$ and $y(t)$ being the two dof). Similar normal modes of two dof system are also investigated in [11], where the power of nonlinearity was assumed to be any real number. Also a three dof in considered, too. The extension to more dof and continuous systems is reported in [12], where the examples are up to N=5, and for the case of the beam the separation of variables is exploited.

In all previous works only similar normal modes are considered, i.e. $y_i = c_i\,x,\ i = 1, 2, ..., N$. This latter hypothesis is very strong, since it restricts that much the system outcome, and practically entails considering only the "main"

dof x. The relaxation of this hypothesis is the goal of this paper, where two coupled Duffing oscillators are considered and *generic*, *non similar*, solutions are investigated. Actually, I also do not focus on the nonlinear normal mode framework [13, 14], and consider instead the full system dynamics not necessarily restricting to manifolds.

This extension is far from trivial, from the one side, and allows us to investigate more systems behaviours, from the other side, thus paving the way to new applications with the benefits of having a closed form solution to deals with them. In any case, all current applications my benefit from having an exact solution, and the advantage becomes larger and larger as, for example, the excitation amplitude increases and available approximate solutions become unreliable.

Coupled Duffing oscillators have been previously studied. In [15] a tree of periodic solutions up to chaos were studied. In [16] attention was focused on route to chaos and numerical solutions were considered, while [17] was devoted to the synchronization between different degrees of freedom. Transient chaos have been investigated numerically and experimentally in [18] in the case of negative linear stiffness, i.e. double wells potential, without external excitation. In [19] a perturbation approach has been used to obtain an approximate solution. The multiple time scale method has been employed in [20] to investigated the 1:1 internal resonance and in [21] to obtain approximate analytical results to be compared with experimental results. The Krylov–Bogoliubov–Mitropolsky method has been instead utilized in [22, 23] to obtain some interesting properties of the frequency response curves.

Numerical simulations have been compared with experimental results obtained on an electrical device in [24] in the case without external excitation, with the aim of studying the effect of the (linear) coupling on the onset of oscillations. In [25] the numerically obtained frequency response curves (with damping and excitation) are compared with the analytically determined backbone curves (without damping and excitation).

In all previous works the excitation, when present, was always harmonic, and no attempts has been done to obtain an exact, closed form analytical solution, which is the goal on this work.

This paper is organized as follow. In Sect. 2 the coupled Duffing oscillators are introduced, and the solution technique is illustrated in detail. The analytical findings are illustrated with some examples in Sect. 3, where some interesting dynamical phenomena are reported. Finally, the paper ends with some conclusions and suggestions for further developments (Sect. 4).

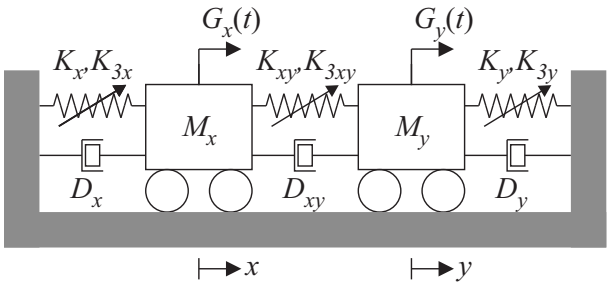

Figure 1: A schematic mechanical drawing of the considered two dof nonlinear system.

2 Theoretical developments

2.1 Coupled Duffing oscillators

Let us consider the two linearly and nonlinearly coupled, damped and forced Duffing oscillators schematically illustrated in Fig. 1. This is the same system studied in [25] with a different approach.

The equations of motion are

$$\begin{aligned} M_x\ddot{x} + D_x\dot{x} + K_x x + K_{3x}x^3 + D_{xy}(\dot{x}-\dot{y}) + K_{xy}(x-y) + K_{3xy}(x-y)^3 = G_x(t), \\ M_y\ddot{y} + D_y\dot{y} + K_y y + K_{3y}y^3 + D_{xy}(\dot{y}-\dot{x}) + K_{xy}(y-x) + K_{3xy}(y-x)^3 = G_y(t). \end{aligned} \tag{1}$$

It is worth to note that, because of the coupling terms K_{xy}, K_{3xy} and D_{xy}, a monomodal solution (e.g., $x \neq 0$ and $y = 0$) is not possible in general (unless, e.g., $G_y(t) = -(D_{xy}\dot{x} + K_{xy}x + K_{3xy}x^3)$).

The two (circular) natural frequencies $\omega_{1,2}$ of (1), that are computed by solving the undamped unforced linear part of (1),

$$\begin{aligned} M_x\ddot{x} + K_x x + K_{xy}(x-y) = 0, \\ M_y\ddot{y} + K_y y + K_{xy}(y-x) = 0, \end{aligned} \tag{2}$$

are given by $\omega_{1,2} = \sqrt{\rho_{1,2}}$, where $\rho_{1,2}$ are the two solutions of the second order algebraic equation

$$\rho^2 - \left[\omega_x^2 + \omega_y^2 + K_{xy}\left(\frac{1}{M_x} + \frac{1}{M_y}\right)\right]\rho + \left[\omega_x^2\omega_y^2 + K_{xy}\left(\frac{\omega_y^2}{M_x} + \frac{\omega_x^2}{M_y}\right)\right] = 0, \tag{3}$$

where

$$\omega_x = \sqrt{\frac{K_x}{M_x}}, \quad \omega_x = \sqrt{\frac{K_y}{M_y}}. \tag{4}$$

They differ from ω_x and ω_y because of the linear coupling K_{xy}.

I assume that, in the absence of the external load ($G_x = G_y = 0$), the rest position $x = y = 0$ has linear oscillations in its neighborhood, i.e. I assume that ω_1 and ω_2 are real (and positive). The damping coefficients are also non negative, $D_x \geq 0$, $D_y \geq 0$ and $D_{xy} \geq 0$, but I implicitly assume that they are small, according to what happen in commmon practical applications described by (1). However, the smallness of D_x, D_y and D_{xy} is not used in the following mathematical passages, and thus it is not really requested. The nonlinear stiffnesses K_{3x}, K_{3y} and K_{3xy}, on the other hand, can have arbitrary signs.

The potential associated to (1) is

$$P = K_x \frac{x^2}{2} + K_y \frac{y^2}{2} + K_{3x} \frac{x^4}{4} + K_{3y} \frac{y^4}{4} + K_{xy} \frac{(x-y)^2}{2} + K_{3xy} \frac{(x-y)^4}{4}. \tag{5}$$

2.2 Exact solution

Extending the ideas of Hsu [4] I assume that the excitations $G_x(t)$ and $G_y(t)$ have the following expressions

$$\begin{aligned} G_x &= D_x \dot{x} + D_{xy}(\dot{x} - \dot{y}) + K_{xy}(x-y) + K_{3xy}(x-y)^3 - S_x x - S_{3x} x^3, \\ G_y &= D_y \dot{y} + D_{xy}(\dot{y} - \dot{x}) + K_{xy}(y-x) + K_{3xy}(y-x)^3 - S_y y - S_{3x} y^3, \end{aligned} \tag{6}$$

where S_x, S_{3x}, S_y and S_{3y} are free parameters to be determined later on to "shape" the excitation.

Inserting (6) in (1) one gets

$$\begin{aligned} \ddot{x} + (\omega_x^2 + W_x)x + (k_x + C_x)x^3 = 0, \\ \ddot{y} + (\omega_y^2 + W_y)y + (k_y + C_y)y^3 = 0, \end{aligned} \tag{7}$$

where

$$\begin{aligned} W_x = \frac{S_x}{M_x}, \quad k_x = \frac{K_{3x}}{M_x}, \quad C_x = \frac{S_{3x}}{M_x}, \\ W_y = \frac{S_y}{M_y}, \quad k_y = \frac{K_{3y}}{M_y}, \quad C_y = \frac{S_{3y}}{M_y}. \end{aligned} \tag{8}$$

The solutions of (7) starting from the initial conditions

$$x(0) = A_x, \quad \dot{x}(0) = 0, \quad y(0) = A_y, \quad \dot{y}(0) = 0, \tag{9}$$

are

$$\begin{aligned} x(t) = A_x \, cn(a_x t, b_x), \\ y(t) = A_y \, cn(a_y t, b_y), \end{aligned} \tag{10}$$

where

$$
\begin{aligned}
a_x^2 &= A_x^2(k_x + C_x) + (\omega_x^2 + W_x),\\
b_x^2 &= \frac{A_x^2(k_x + C_x)}{2a_x^2},\\
a_y^2 &= A_y^2(k_y + C_y) + (\omega_y^2 + W_y),\\
b_y^2 &= \frac{A_y^2(k_y + C_y)}{2a_y^2},
\end{aligned}
\tag{11}
$$

and where "*cn*" is the Jacobian elliptic function [6]. Note that A_x and A_y are the amplitudes of the oscillations, and are *not* requested to be positive. In fact, e.g., $A_x > 0$ and $A_y < 0$ means that $x(t)$ and $y(t)$ are in counter phase. We are not considering arbitrary phase shift between the two dof, which can be taken into account by assuming, for example, $x(t) = A_x\, cn(a_x t + \varphi, b_x)$. The case $\varphi \neq 0$, that certainly will provide some further insight, is left for future developments.

According to [6] (see also [26], Chap. 16), the period of the function $cn(u, m)$ is given by $T = 4K(m)$. Thus, the periods of the solutions $x(t)$ and $y(t)$ are

$$
\begin{aligned}
T_x &= \frac{4K(b_x)}{a_x} = \frac{4}{a_x} K\left(\frac{|A_x|\sqrt{k_x + C_x}}{a_x\sqrt{2}}\right) = \frac{4\sqrt{2}\, b_x}{|A_x|\sqrt{k_x + C_x}} K(b_x),\\
T_y &= \frac{4K(b_y)}{a_y} = \frac{4}{a_y} K\left(\frac{|A_y|\sqrt{k_y + C_y}}{a_y\sqrt{2}}\right) = \frac{4\sqrt{2}\, b_y}{|A_y|\sqrt{k_y + C_y}} K(b_y),
\end{aligned}
\tag{12}
$$

where $K(x)$ is the complete elliptic integral of the first kind [6] and is illustrated in Fig. 2. Note that it is defined only for $-1 < b_x < 1$.

The (circular) frequencies are $\Omega_x = 2\,\pi/T_x$ and $\Omega_y = 2\,\pi/T_y$. For small values of the amplitudes the following asymptotic developments holds

$$
\begin{aligned}
\Omega_x &= \sqrt{\omega_x^2 + W_x}\left[1 + \frac{3}{8}\frac{k_x + C_x}{\omega_x^2 + W_x} A_x^2 - \frac{21}{256}\left(\frac{k_x + C_x}{\omega_x^2 + W_x}\right)^2 A_x^4\right.\\
&\left. + \frac{81}{2048}\left(\frac{k_x + C_x}{\omega_x^2 + W_x}\right)^3 A_x^6 + ...\right],\\
\Omega_y &= \sqrt{\omega_y^2 + W_y}\left[1 + \frac{3}{8}\frac{k_y + C_y}{\omega_y^2 + W_y} A_y^2 - \frac{21}{256}\left(\frac{k_y + C_y}{\omega_y^2 + W_y}\right)^2 A_y^4\right.\\
&\left. + \frac{81}{2048}\left(\frac{k_y + C_y}{\omega_y^2 + W_y}\right)^3 A_y^6 + ...\right].
\end{aligned}
\tag{13}
$$

As parameters measuring the amplitude of the excitation I choose

$$
\begin{aligned}
F_x &= G_x(0) = K_{xy}(A_x - A_y) + K_{3xy}(A_x - A_y)^3 - M_x A_x(W_x + C_x A_x^2),\\
F_y &= G_y(0) = K_{xy}(A_y - A_x) + K_{3xy}(A_y - A_x)^3 - M_y A_y(W_y + C_y A_y^2).
\end{aligned}
\tag{14}
$$

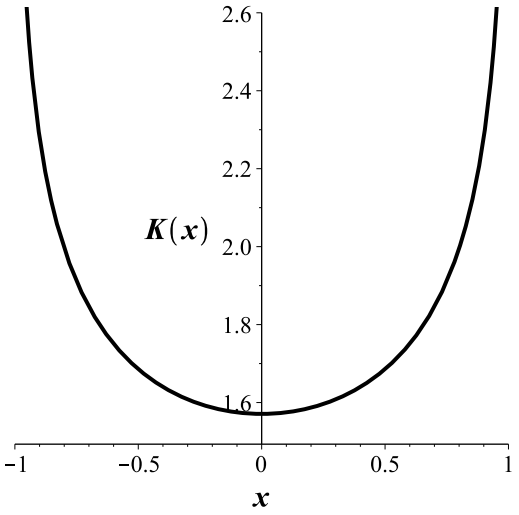

Figure 2: The function $K(x)$.

Since $\dot{x}(0) = \dot{y}(0) = 0$, the damping terms D_x, D_y and D_{xy} do not appear in (14), although they affect the excitations. The implicit assumption that they are small suggests that this is not a problem.

The parameters F_x and F_y are proportional to the maximum value of $G_x(t)$ and $G_y(t)$. In fact,

$$\begin{aligned}
\dot{G}_x(0) &= -D_x A_x a_x^2 - D_{xy}(A_x a_x^2 - A_y a_y^2),\\
\dot{G}_y(0) &= -D_y A_y a_y^2 - D_{xy}(A_y a_y^2 - A_x a_x^2),\\
\ddot{G}_x(0) &= -(A_x a_x^2 - A_y a_y^2)[K_{xy} + 3K_{3xy}(A_x - A_y)^2] + M_x A_x a_x^2 (W_x + 3C_x A_x^2),\\
\ddot{G}_y(0) &= -(A_y a_y^2 - A_x a_x^2)[K_{xy} + 3K_{3xy}(A_y - A_x)^2] + M_y A_y a_y^2 (W_y + 3C_y A_y^2),
\end{aligned} \tag{15}$$

so that when $D_x = D_y = D_{xy} = 0$ and simultaneously $A_x \ddot{G}_x(0) < 0$ and $A_y \ddot{G}_y(0) < 0$, F_x and F_y are exactly the maximum/minimimum of $G_x(t)$ and $G_y(t)$, respectively.

Solving (14) with respect to W_x and W_y one obtains

$$\begin{aligned}
W_x &= \frac{K_{xy}(A_x - A_y) + K_{3xy}(A_x - A_y)^3 - C_x M_x A_x^3 - F_x}{M_x\, A_x},\\
W_y &= \frac{K_{xy}(A_y - A_x) + K_{3xy}(A_y - A_x)^3 - C_y M_y A_y^3 - F_y}{M_y\, A_y}.
\end{aligned} \tag{16}$$

Inserting (16) in (18) one gets

$$a_x^2 = \frac{K_{3xy}(A_x - A_y)^3 + K_{xy}(A_x - A_y)}{M_x\, A_x} + k_x A_x^2 + \omega_x^2 - \frac{F_x}{M_x\, A_x},$$
$$a_y^2 = \frac{K_{3xy}(A_y - A_x)^3 + K_{xy}(A_y - A_x)}{M_y\, A_y} + k_y A_y^2 + \omega_y^2 - \frac{F_y}{M_y\, A_y}, \qquad (17)$$

and then

$$b_x^2 = \frac{M_x A_x^3 (k_x + C_x)}{2\left[K_{3xy}(A_x - A_y)^3 + K_{xy}(A_x - A_y) + M_x A_x (k_x A_x^2 + \omega_x^2) - F_x\right]},$$
$$b_y^2 = \frac{M_y A_y^3 (k_y + C_y)}{2\left[K_{3xy}(A_y - A_x)^3 + K_{xy}(A_y - A_x) + M_y A_y (k_y A_y^2 + \omega_y^2) - F_y\right]}. \qquad (18)$$

When T_x and T_y are incommensurable the excitations $G_x(t)$ and $G_y(t)$ are *not* periodic because $x-y$ is not periodic, see (6). When T_x and T_y are commensurable, i.e. when $\exists\, m, n \in \mathbb{N}$ such that $n\, T_x = m\, T_y$, then $G_x(t)$ and $G_y(t)$ are periodic with the same period $T = n\, T_x = m\, T_y$. In this paper I am interested in the simplest case $n = m = 1$, which also entails that $x(t)$ and $y(t)$ have the *same* period. In fact, when $T_x = T_y = T$ all the four functions $G_x(t)$, $G_y(t)$, $x(t)$ and $y(t)$ have period T. The cases $n = m \neq 1$ and $n \neq m$ are interesting and are left for future works.

From (12) the condition $T_x = T_y$ requires

$$\frac{b_x}{|A_x|\sqrt{k_x + C_x}} K(b_x) = \frac{b_y}{|A_y|\sqrt{k_y + C_y}} K(b_y), \qquad (19)$$

or

$$\lambda b_x K(b_x) = b_y K(b_y), \qquad \lambda = \frac{|A_y|\sqrt{k_y + C_y}}{|A_x|\sqrt{k_x + C_x}}. \qquad (20)$$

Note that if (b_x, b_y) is a solution for a given λ, also $(-b_x, -b_y)$ is a solution for that λ and (b_y, b_x) is a solution for $1/\lambda$. The solutions of (20) in terms of b_x and b_y for different values of λ are illustrated in Fig. 3.

Given all the other parameters (remember the expressions of b_x and b_y given by (18)), and in particular the excitation amplitudes F_x and F_y, equation (20) links the amplitudes A_x and A_y of the two oscillations $x(t)$ and $y(t)$, and thus can be named "coupling equation". Roughly speaking, it practically identifies the nonlinear normal mode, even if this interesting topic is not further discussed.

The solution is then obtained according to the following steps:

- solve (19), which is a nonlinear algebraic equation that can be easily solved numerically, to obtain, for example, $A_y(A_x)$;
- insert this expression in (12)-(17) to obtain $T(A_x)$ ($T = T_x = T_y$);

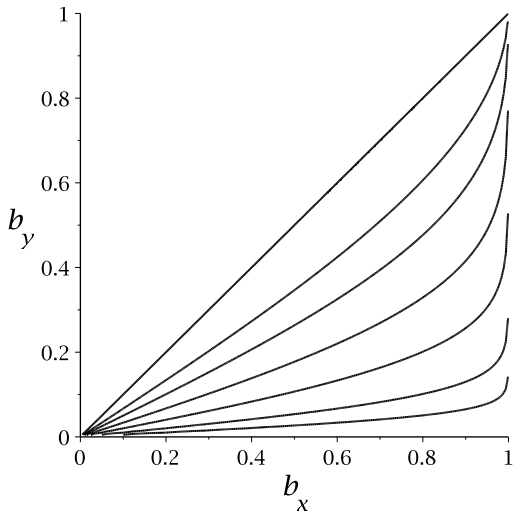

Figure 3: The solution of (20) for $\lambda = 1$ (top - the linear one); 1.5; 2; 3; 5; 10; 20 (bottom).

- invert this expression to obtain $A_x(T)$;
- compute $A_y(A_x(T)) = A_y(T)$.

Alternatively to the procedure illustrated above, one can fix the period T and then solve the two nonlinear algebraic equations $T = T_x$ and $T = T_y$ in the two unknowns A_x and A_y. This is more demanding from a numerical point view, but can be useful if one is interested in one period only.

The functions $A_x(T)$ and $A_y(T)$ provide the amplitude of the oscillations as a function of the period of the excitation (and of the response, indeed) and of the excitation amplitudes (F_x and F_y), thus giving the frequency response curves. They will depend also on the parameters of the equations and on the parameters C_x and C_y, that can be chosen freely.

Sometimes it is preferred to use the circular frequency $\Omega = 2\pi/T$ instead of T as a driving parameter. Obtaining $A_x(\Omega)$ and $A_y(\Omega)$ is then trivial.

It is worth the remark that with the proposed approach there are no extra efforts to deals with the internal resonance case, contrarily to what happens, for example, with asymptotic methods.

2.3 Admissibility of the coupling equation

The solutions of the coupling equation (19) are discussed. From Fig. 1 it is noted that the solution exists only if

$$b_x^2 < 1, \quad b_y^2 < 1, \tag{21}$$

that delimitate two regions $R_{1,2}$ in the (A_x, A_y) plane.

Furthermore, it is also needed that

$$\frac{b_x^2}{k_x + C_x} > 0, \quad \frac{b_y^2}{k_y + C_y} > 0, \tag{22}$$

otherwise the period would not be real, see (12). They bound two other regions $R_{3,4}$ in the (A_x, A_y) plane. Solutions exist only in the intersection of these four regions. This permits to delimitate the region were to look for a physical solution in the plane (A_x, A_y).

An example of the four regions and of their intersection is reported in Fig. 4. Note that in principle it is possible to have both in phase (A_x and A_y having the same sign) and out of phase (A_x and A_y with different sign) solutions.

2.4 Stability

To study the stability of a given periodic solutions, the Floquet method has been employed. The first step is to compute the monodromy matrix M.

Given the initial conditions $(x(0), \dot{x}(0), y(0), \dot{y}(0)) = (A_x, 0, A_y, 0)$ (see (9)) and keeping fixed the excitation, I consider small perturbations in all the four directions of the phase space, and integrate numerically the equations (1) from $t = 0$ to $t = T$, obtaining a numerical approximation of the components of M:

$$\begin{aligned}
&(x(0), \dot{x}(0), y(0), \dot{y}(0)) = (A_x + d, 0, A_y, 0) \to (x(T), \dot{x}(T), y(T), \dot{y}(T)) \\
&M_{11} = \frac{x(T) - x(0)}{d}, M_{12} = \frac{\dot{x}(T) - \dot{x}(0)}{d}, M_{13} = \frac{y(T) - y(0)}{d}, M_{14} = \frac{\dot{y}(T) - \dot{y}(0)}{d}; \\
&(x(0), \dot{x}(0), y(0), \dot{y}(0)) = (A_x, d, A_y, 0) \to (x(T), \dot{x}(T), y(T), \dot{y}(T)) \\
&M_{21} = \frac{x(T) - x(0)}{d}, M_{22} = \frac{\dot{x}(T) - \dot{x}(0)}{d}, M_{23} = \frac{y(T) - y(0)}{d}, M_{24} = \frac{\dot{y}(T) - \dot{y}(0)}{d}; \\
&(x(0), \dot{x}(0), y(0), \dot{y}(0)) = (A_x, 0, A_y + d, 0) \to (x(T), \dot{x}(T), y(T), \dot{y}(T)) \\
&M_{31} = \frac{x(T) - x(0)}{d}, M_{32} = \frac{\dot{x}(T) - \dot{x}(0)}{d}, M_{33} = \frac{y(T) - y(0)}{d}, M_{34} = \frac{\dot{y}(T) - \dot{y}(0)}{d}; \\
&(x(0), \dot{x}(0), y(0), \dot{y}(0)) = (A_x, 0, A_y, d) \to (x(T), \dot{x}(T), y(T), \dot{y}(T)) \\
&M_{41} = \frac{x(T) - x(0)}{d}, M_{42} = \frac{\dot{x}(T) - \dot{x}(0)}{d}, M_{43} = \frac{y(T) - y(0)}{d}, M_{44} = \frac{\dot{y}(T) - \dot{y}(0)}{d}.
\end{aligned} \tag{23}$$

The number d needs to be small enough to stabilize the numerical results, but cannot be to small to not face with round-off problems. I have done a preliminary convergence check, and I have found that $d = 0.0001$ gives adequate accuracy in all forthcoming examples.

Then, the eigenvalue of the 4×4 matrix M are computed. If the modulus of all eigenvalues is lesser than 1 the oscillation is stable; if at least one eigenvalue has modulus grater than 1 the solution is unstable. The case in which one (or more)

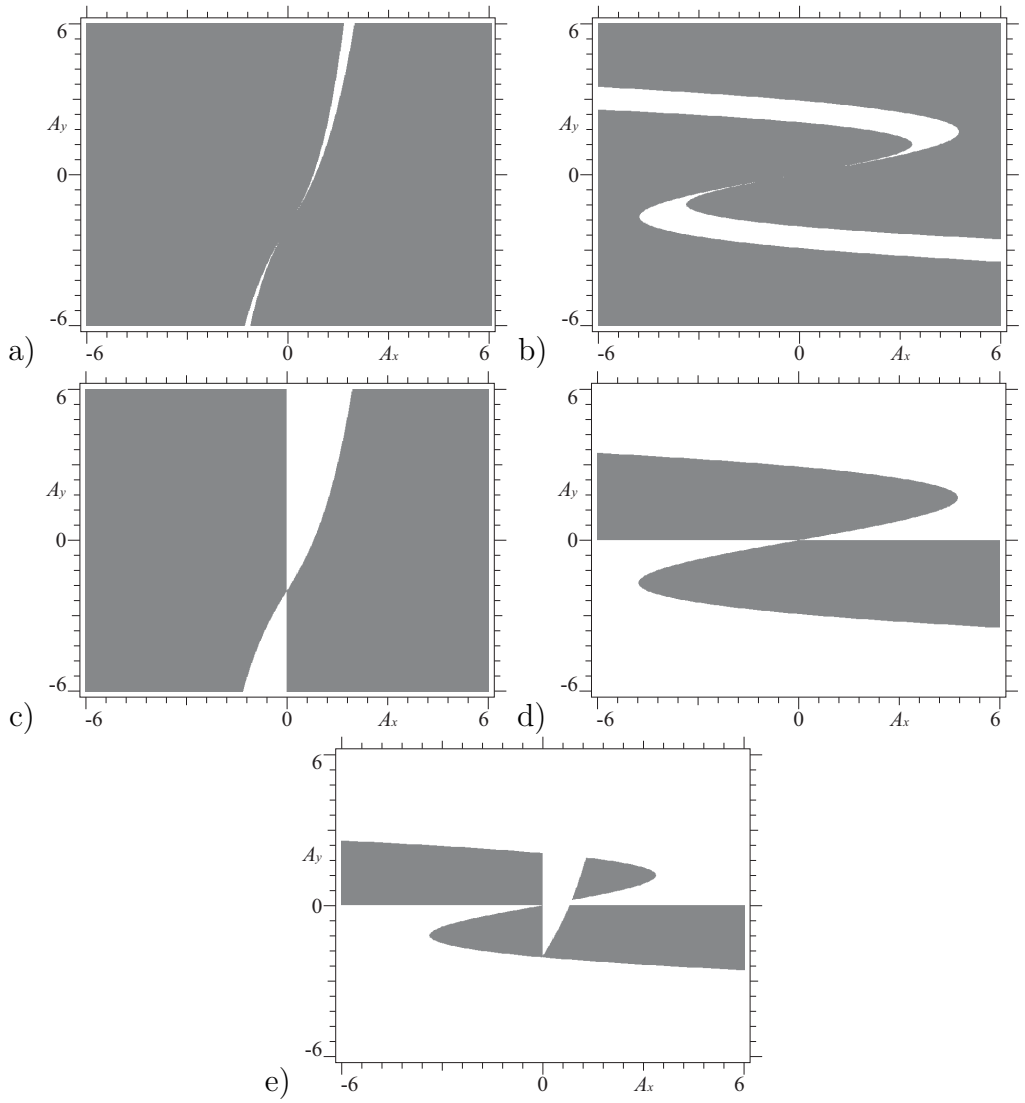

Figure 4: The four regions. a) R_1, b) R_2, c) R_3, d) R_4 and e) their intersection, where the solutions are located. $M_x = 1$, $D_x = 0$, $\omega_x = 1.1$, $k_x = 1$, $M_x = 1$, $D_y = 0$, $\omega_y = 1.8$, $k_y = -1$, $D_{xy} = 0$, $K_{xy} = 1$, $K_{3xy} = 0$, $C_x = 0$, $C_y = 0$, $F_x = 2$, $F_y = 0$.

eigenvalues has (have) modulus equal to 1 would require deeper analysis. Since however this case does not involve exponential divergence, I name it "stable", even if this is not properly correct from a mathematical point of view, but likely enough for practical applications.

For example, the four eigenvalues of the solution reported in the forthcoming Fig. 9a are $-0.3228 \pm i\,0.9465$ and $-0.9047 \pm i\,0.42597$. Each has modulus 1 (as a consequence of the fact that there is no damping in that case) and thus it is stable.

The monodromy matrix has been computed numerically. Attempts to compute it analytically, that look quite difficult, are left for further developments.

3 Results

In this section the different behaviours exhibited by the system for various values of the parameters are shown. The next examples are reported with the aim of showing the system outcome far (examples 1 and 2) and close (example 3) to the internal resonance, for hardening vs softening (examples 1 and 3) and both hardening (example 2) behaviour of the two dof. Also linear (examples 1 and 2) and nonlinear (example 3) coupling stiffnesses are considered. The effect of the increasing amplitude is also shown (example 1). A validation against results of the literature are also reported in the ex. 4.

To simplify the description I assume unitary masses $M_x = M_y = 1$ (as in [25]). Furthermore, in the main examples I consider excitation on one dof only, i.e. $F_x \neq 0$ and $F_y = 0$, and the undamped case, $D_x = D_y = D_{xy} = 0$. I have checked that small damping coefficients (up to $D_i = 0.01$) does not change significatively the reported results. I also initially do not exploit the free excitation parameter C_x and C_y, i.e. $C_x = C_y = 0$. The only parameters that are varied are ω_x, ω_y, k_x, k_y, K_{xy}, K_{3xy} and F_x.

The first example is

$$\omega_x = 1.1, \quad k_x = 1, \quad \omega_y = 1.8, \quad k_y = -1, \quad K_{xy} = 1, \quad K_{3xy} = 0, \tag{24}$$

for increasing values of F_x. The two natural frequencies are $\omega_1 = 1.3417$ and $\omega_2 = 2.1563$, and thus this case is far from internal resonance. The coupling is only linear, since $K_{3xy} = 0$. The x dof is hardening ($k_x > 0$) while the y one is softening ($k_y < 0$). This is better appreciated in the contourplot of the potential, which is reported in Fig. 5. The potential well is clearly visible, and is delimited by the two saddles $(\pm 0.7210; \pm 1.9682)$.

The solutions for $F_x = 0.5; 1.0; 2.0$ are reported in Figs. 6-8, respectively.

The most relevant aspect is that there are three disjoint branches of solution, see Figs. 6c, 7c and 8c, that are reported with different colors, both in-phase ($A_x\, A_y > 0$) and out-of-phase ($A_x\, A_y < 0$).

The main hardening path of A_x is clearly visible in all cases (Figs. 6a, 7a and 8a), and extends up to large amplitudes. Also the softening path of A_y is well

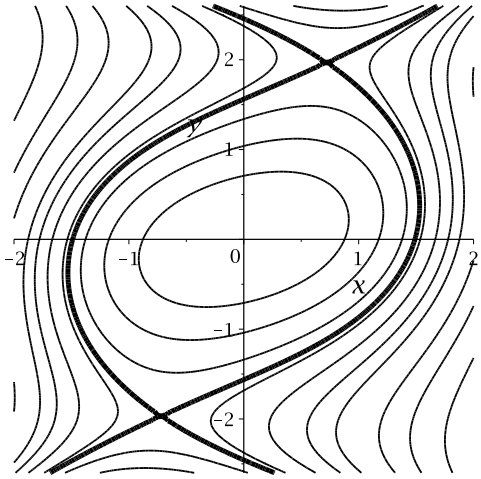

Figure 5: The contour plot of the potential (5) for the parameter values (24). Thick lines correspond to the separatrixes (heteroclinic orbits) surrounding the unique potential well.

recognizable, although it reaches lower amplitudes, basically because at that level the y goes out of the potential well (see Fig. 5 and note that the potential well ends at $y = 1.9682$).

The blue path is mainly relevant for the x variable, and the black one for the y. They have the classical behavior of the nonlinear frequency response curves, i.e. they have a double branch in the (Ω, A) parameters space, with the lowest stable and the upper unstable. They are not qualitatively modified by increasing the excitation amplitude.

The red path, on the other hand, takes into account the coupling. For low values of F_x there are two distinct peaks in the red frequency response curve, with a "valley" in between, which is particularly visible in Fig. 6b around $\Omega = 1.8$. The stability is lost by classical saddle-node bifurcations. The red path has a important branch in the $A_x < 0$ and $A_y < 0$ part of Fig. 6c, which is somehow specular to the black path.

By increasing F_x the depth of the valley reduces (see Fig. 7b), as well as the range in which it is stable. In Fig. 7c also the branch belonging to $A_x < 0$ and $A_y < 0$ shrinks.

For $F_x = 2$ the main element of novelty is that the valley of the red path disappears; this path also disappears from the $A_x < 0$ and $A_y < 0$ part of Fig. 8c, and becomes a monotonic function in all the three pictures of Fig. 8, with a geometrically simpler behaviour. However, the legacy of the previous more complex behaviour is seen in the intermittence of unstable and stable intervals, which is a characteristic of this case.

For $\Omega = 1.6234$ ($T = 3.8705$) the unique solution is $A_x = 1.0$, $A_y = -1.6842$

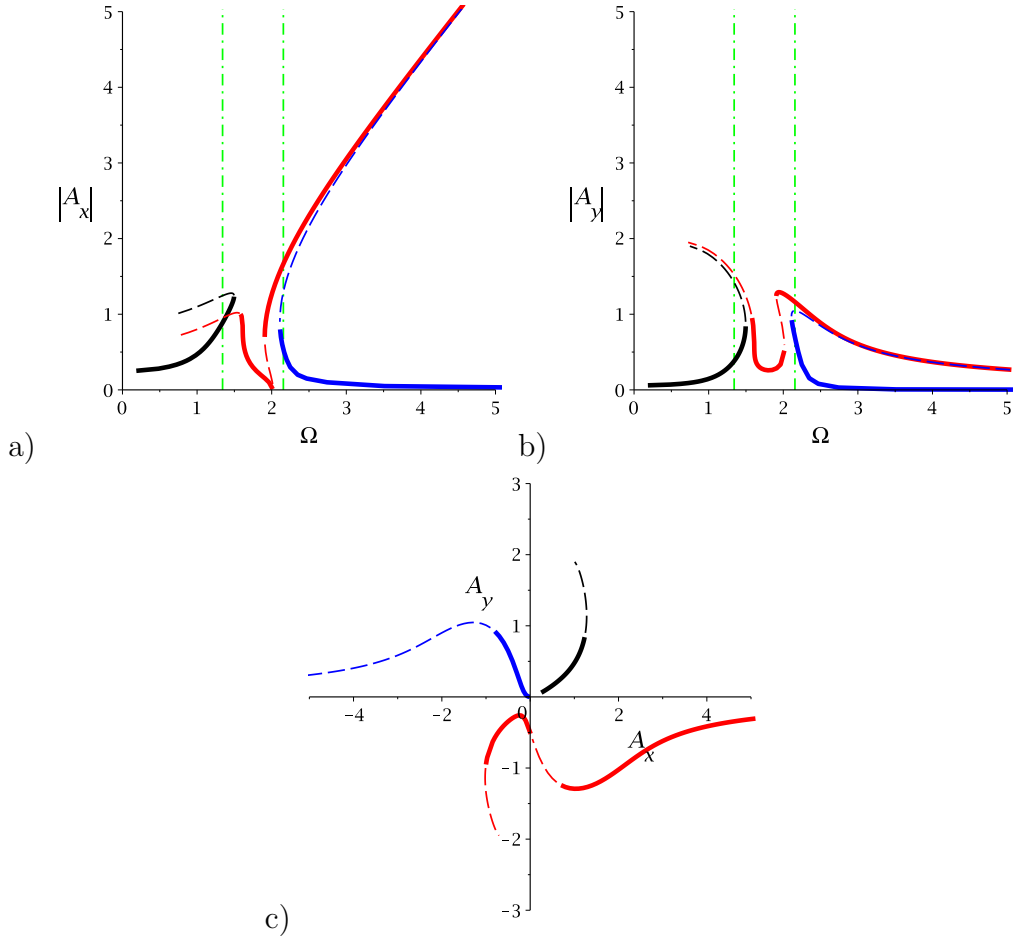

Figure 6: The solution for $F_x = 0.5, \omega_x = 1.1, k_x = 1, \omega_y = 1.8, k_y = -1, K_{xy} = 1, K_{3xy} = 0, C_x = 0, C_y = 0$. Dashdot green lines are in correspondence of the two natural frequencies; solid thick lines are stable solutions; dashed thin lines are unstable solutions.

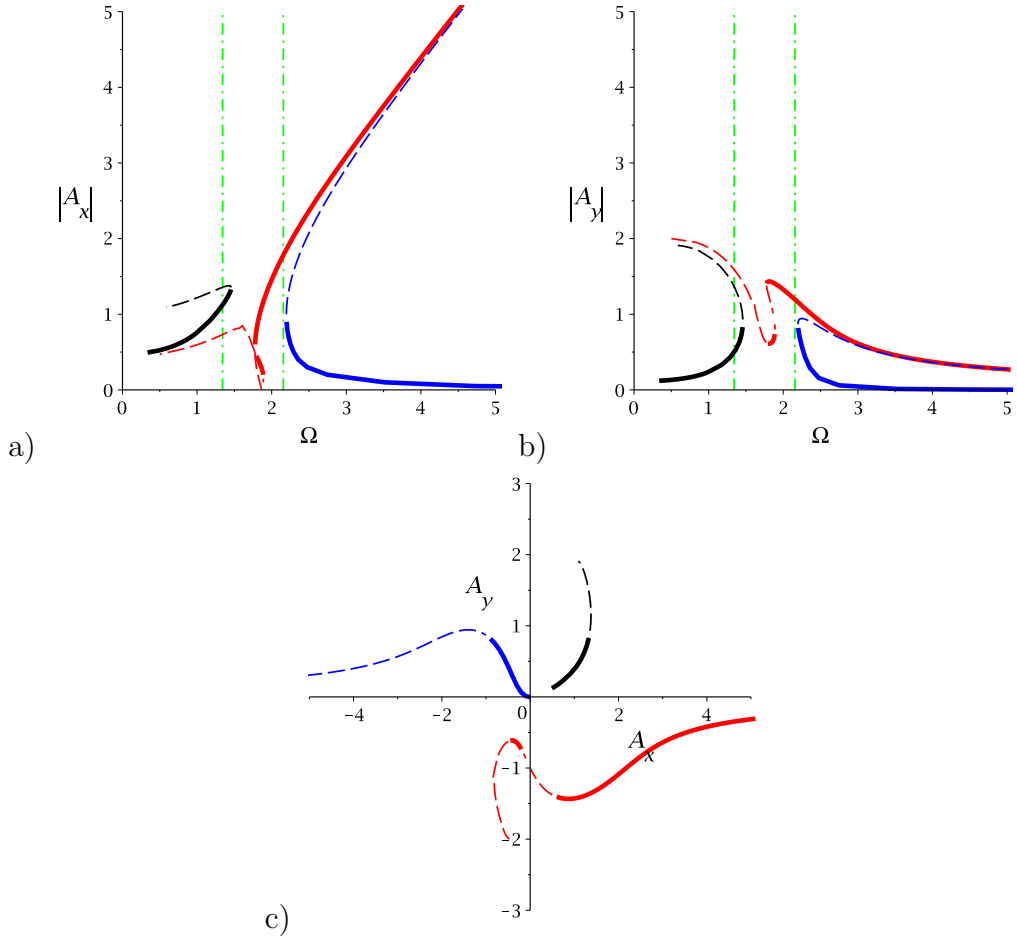

Figure 7: The solution for $F_x = 1.0, \omega_x = 1.1, k_x = 1, \omega_y = 1.8, k_y = -1, K_{xy} = 1, K_{3xy} = 0, C_x = 0, C_y = 0$. Dashdot green lines are in correspondence of the two natural frequencies; solid thick lines are stable solutions; dashed thin lines are unstable solutions.

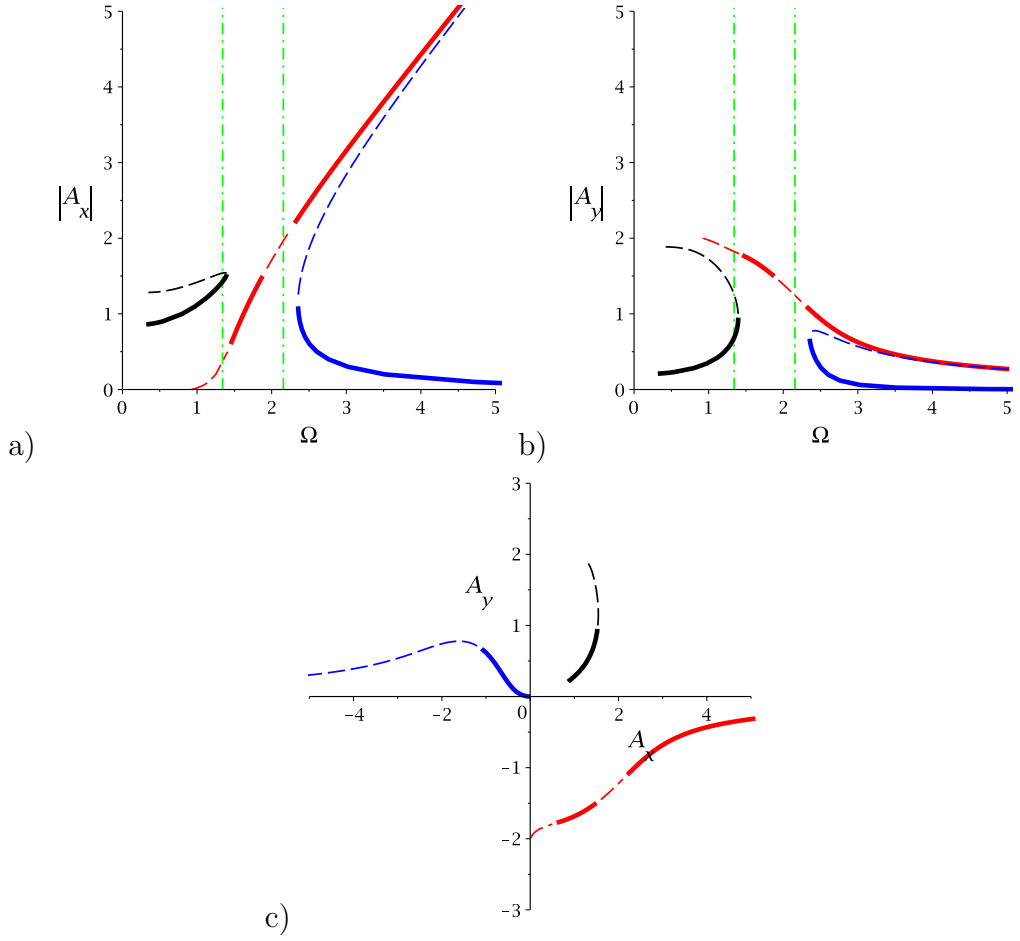

Figure 8: The solution for $F_x = 2.0, \omega_x = 1.1, k_x = 1, \omega_y = 1.8, k_y = -1, K_{xy} = 1, K_{3xy} = 0, C_x = 0, C_y = 0$. Dashdot green lines are in correspondence of the two natural frequencies; solid thick lines are stable solutions; dashed thin lines are unstable solutions. The circles correspond to the case of Fig. 9a,b.

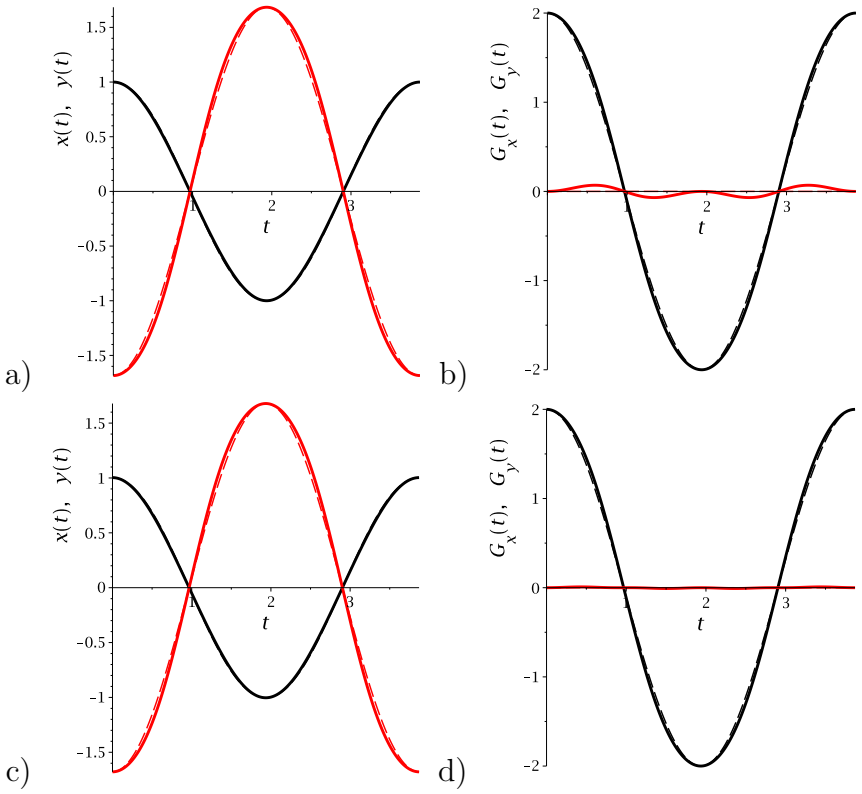

Figure 9: $x(t)$ (black) and $y(t)$ (red); $G_x(t)$ (black) and $G_y(t)$ (red) for $F_x = 2, F_y = 0, \xi_x = 0, \omega_x = 1.1, k_x = 1, \xi_y = 0, \omega_y = 1.8, k_y = -1, K_{xy} = 1, C_x = 0, \Omega = 1.6234$. The dashed curves are the cosine functions with the same amplitude and period. a,b) C_y=0; c,d) $C_y = 0.035$.

(see Fig. 8). The time histories of $x(t)$ and $y(t)$ are practically cosine functions, as shown in Fig. 9a. Also $G_x(t)$ is practically a cosine function (Fig. 9b, black).

It is noted that $G_y(t)$ is not null (Fig. 9b, red), in spite of the assumption $F_y = 0$, because of the different shapes of $x(t)$ and $y(t)$. It is very small ($f_{x,\max} = 0.0692$, about 3.4% of the amplitude $F_x = 2$) and can be enough for practically purposes. If however one needs to reduce it further more, it is possible to use the free parameter C_y. For example, for $C_y = 0.035$ (i.e. with a very minor "cost") $G_y(t)$ strongly reduces and practically vanishes (see Fig. 10d, red, where $f_{x,\max} = 0.0077$) without affecting in a significant way the other functions $G_x(t)$, $x(t)$ and $y(t)$ (Fig. 9c,d).

The second example,

$$\omega_x = 1.1, \quad k_x = 3, \quad \omega_y = 1.8, \quad k_y = 1, \quad K_{xy} = 1, \quad K_{3xy} = 0, \quad F_x = 2, \quad (25)$$

is obtained by the previous one by changing the nonlinear stiffnesses, that now are

hardening for both dof. Thus, the natural frequencies $\omega_{1,2}$ does not change, while the potential well now has no escape directions.

The corresponding solutions are reported in Fig. 10. They are characterized by 5 different branches, that apparently overlap on Fig. 10a,b but that are indeed distinct, as clearly seen in Fig. 10c.

The hardening behaviour for both x and y, due to $k_x > 0$ and $k_y > 0$, is clearly visible. The black path is always stable, and constitutes the upper one for both dof. The purple path, on the other hand, is always unstable. The three remaining paths have both stable (for low values of the amplitudes) and unstable parts (for high values of the amplitudes), separated by classical saddle-node bifurcations. They exist for $\Omega > \omega_2$.

There are up to four stable coexisting solutions for a fixed value of the excitation frequency. For $\Omega = 3$ they are reported in Fig. 11, which shows that they are quite different between each other, in particular in terms of absolute and relative amplitudes. Again, they are very close to cosine functions.

It is not expected that all attractors of Fig. 11 have the same robustness, namely their basins of attraction could be different in size and shape. A two dimensional cross-section of the basins of attraction of coupled Duffing oscillators have been reported in [27]. This is however not enough to determine the most important attractor, i.e. that with the largest basin of attraction; this requires a detailed dynamical integrity analysis based on fully dimensional basins of attraction, that need complex numerical tools [28]. This is out of the scope of this work and is left for future developments.

In the third example I consider a case in which the coupling is only at the nonlinear level, i.e. $K_{xy} = 0$ and $K_{3xy} \neq 0$. Furthermore, the two frequencies are close, $\omega_1 \cong \omega_2$, namely we are around a 1:1 internal resonance [20]:

$$\omega_x = 1.1, \quad k_x = -3, \quad \omega_y = 1.12, \quad k_y = 1, \quad K_{xy} = 0, \quad K_{3xy} = 1, \quad F_x = 0.1. \tag{26}$$

Internal resonance in coupled oscillators for purposes of mass sensing has been recently exploited, without [30] and with [31] Duffing type cubic nonlinearities.

The frequency response curves are illustrated in Fig. 12. The simultaneous softening for the x variable (because of $k_x < 0$) and hardening for the y variable (because of $k_y > 0$) are clearly visible.

The effect of the nonlinear coupling due to internal resonance manifests has an extra peak (at $\Omega \cong 1.25$) close to the natural frequencies, well visible in Fig. 12b. This peak, that for increasing value of the excitation becomes unstable, has been observed also for other internal resonances [29].

The final fourth example is aimed at reproducing a case from the literature to validate the proposed exact solution. As a matter of fact, it has damping, so that

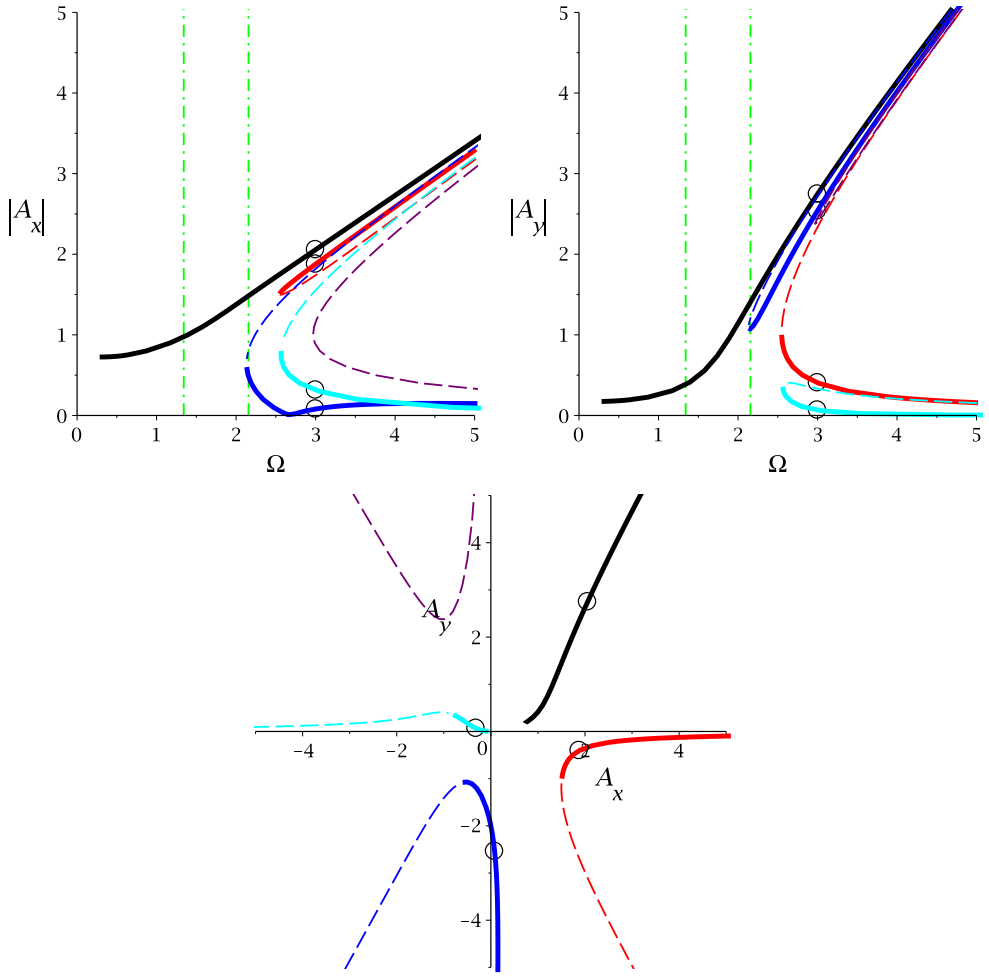

Figure 10: The solution for $F_x = 2, \omega_x = 1.1, k_x = 3, \omega_y = 1.8, k_y = 1, K_{xy} = 1, K_{3xy} = 0, C_x = 0, C_y = 0$. Dashdot green lines are in correspondence of the two natural frequencies; solid thick lines are stable solutions; dashed thin lines are unstable solutions. The circles correspond to the cases of Fig. 11.

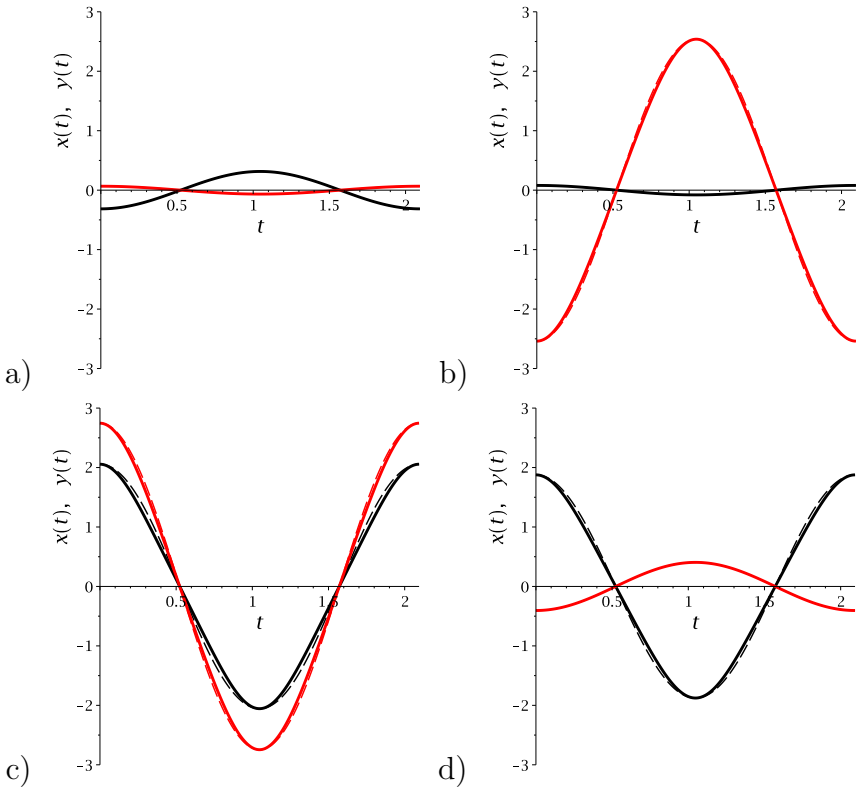

Figure 11: The four coexisting stable solutions for $\Omega = 3$, $x(t)$ (black) and $y(t)$ (red). a) $A_x = -0.3146$ and $A_y = 0.06614$; b) $A_x = 0.07961$ and $A_y = -2.5394$; c) $A_x = 2.0561$ and $A_y = 2.7462$: d) $A_x = 1.8771$ and $A_y = -0.4048$. $F_x = 2, \omega_x = 1.1, k_x = 3, \omega_y = 1.8, k_y = 1, K_{xy} = 1, K_{3xy} = 0, C_x = 0, C_y = 0$. The dashed curves are the cosine functions with the same amplitude and period.

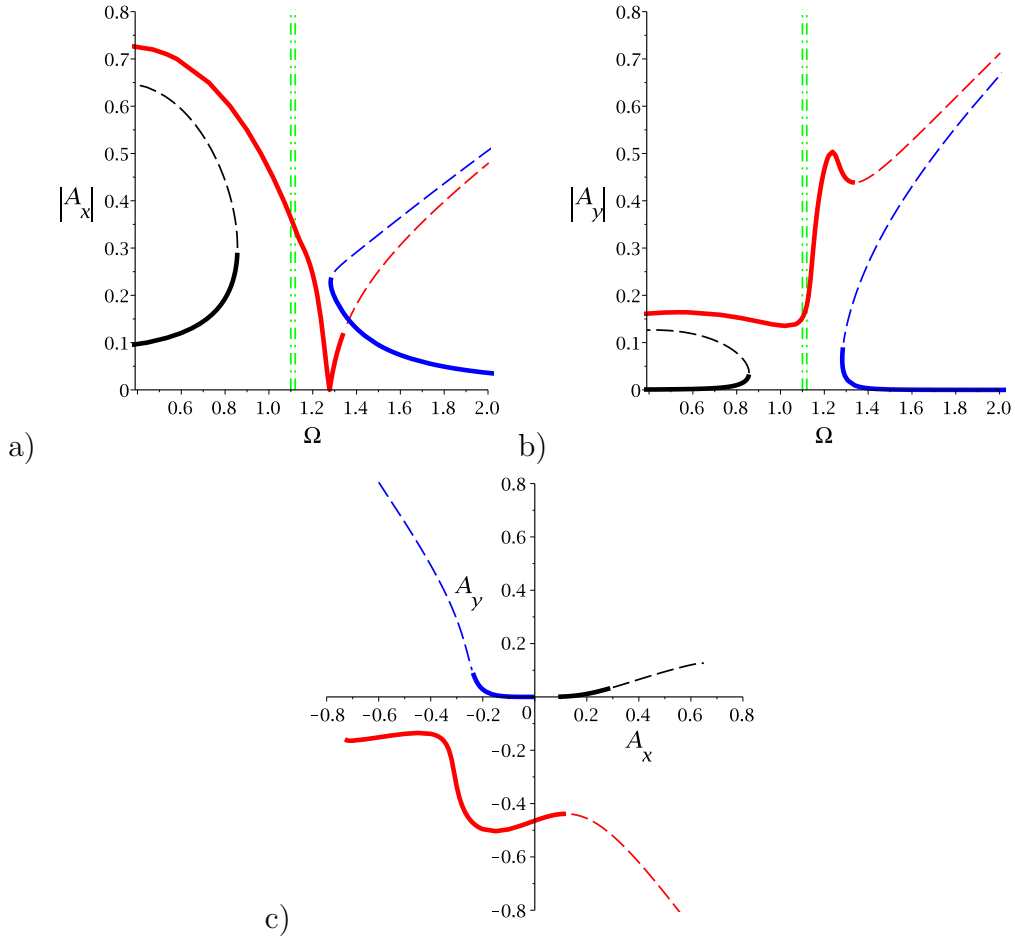

Figure 12: The solution for $F_x = 0.1, \omega_x = 1.1, k_x = -3, \omega_y = 1.12, k_y = 1, K_{xy} = 0, K_{3xy} = 1, C_x = 0, C_y = 0$. Dashdot green lines are in correspondence of the two natural frequencies; solid thick lines are stable solutions; dashed thin lines are unstable solutions.

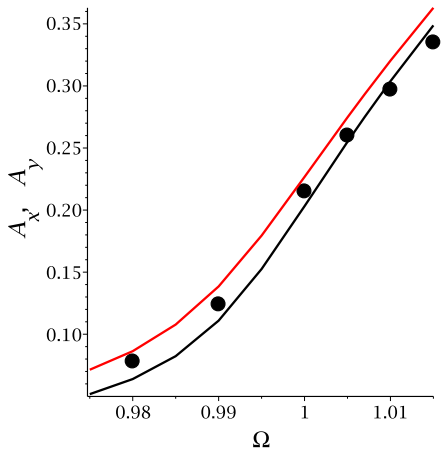

Figure 13: Frequency response curves for fourth example. The continuous lines are present results (black are the amplitude A_x of the first dof, and red the amplitude A_y of the second one). The black circles are the results from [25], where only the amplitude of the first dof is reported.

its effect is preliminarily illustrated, too.

I consider the system studied in [25], which corresponds to $M_x = M_y = 1$, $K_x = K_y = 1$, $K_{xy} = 0.00501252$ (entailing $\omega_1 = 1$ and $\omega_2 = 1.005$), $K_{3x} = K_{3y} = 0.4$, $K_{3xy} = 0.05$, $D_x = D_y = Dxy = 0.008$. Furthermore, I consider what they named "mixed-mode forcing case", where the excitations on the two dof are harmonic with amplitudes 0.0025 and 0.00375, respectively (see their Tab. 1).

The frequency response curves around the natural frequencies are reported in Fig. 13, where they are compared with that of [25] obtained by a purely numerical approach and considering harmonic excitation of the same frequency and the same amplitude. The very good agreement is clearly visible.

For the perfect resonance case $\Omega = 1.0$ the time histories of the responses and of the excitations are reported in Fig. 14. The phase shift between the excitations and the responses, due to damping, is clearly visible. It is equal to 4.6% of the period for G_x and 4.3% for G_y.

4 Conclusions and further developments

To exact solution for the nonlinear oscillations of a system of two coupled Duffing oscillators has been obtained extending a technique developed by Hsu and previously applied only to single dof systems or to similar normal modes. Damping and external excitations have been considered, as well as linear and nonlinear coupling between the two oscillators.

After the analytical developments, where the solution technique has been in-

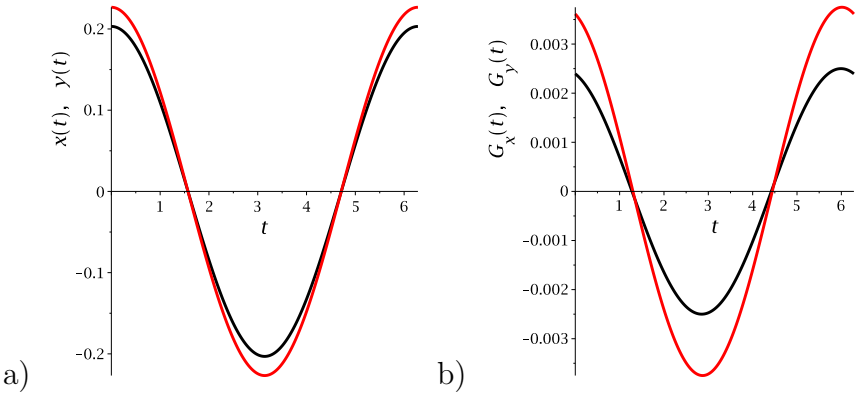

Figure 14: a) $x(t)$ (black) and $y(t)$ (red); b) $G_x(t)$ (black) and $G_y(t)$ (red) for the fourth example when $\Omega = 1$.

troduced and applied to the considered case, the main results have been illustrated with some examples, which have been obtained for different values of the parameters and are aimed at showing some of the possible phenomena in the very rich outcome scenario of the considered system.

Frequency response curves have been reported, and the stability of their branches has been determined by numerically computing the eigenvalues of the monodromy matrix. The effects of linear and nonlinear couplings have been specifically addressed, and a case with internal resonance is considered, too. Also the presence of up to four coexisting attractors has been highlighted.

It is shown that in the considered cases both the system responses and the excitation are very close to classical cosine functions.

There are many directions along which this research can be continued. Among others, the following ones look particularly interesting.

- To continue the parametric investigation to look for other dynamical phenomena, like for example isolated [32], inner [33] or external [34] detached resonance curves;
- to use the free parameters C_x and C_y to design the excitation shape;
- to extend the proposed analytical approach to other systems;
- to consider a generic phase shift between the two dof;
- to consider the case in which the two dof have different periods, possible, possibly different from that of the excitation;
- to consider the case in which T_x and T_y are incommensurable, giving quasi-periodic solutions;
- to consider a parametric instead of an external excitation;

- to study the dynamical integrity of the proposed system;
- to study the analytically the stability of the proposed solutions.

Acknowledgements. The support of the Italian Ministry of University (Italy), under the program "Dipartimento di Eccellenza", is acknowledged. This work is partly done within the "Gruppo Nazionale per la Fisica Matematica" (GNFM) of the INDAM.

References

[1] Lenci S., Clementi F., Mazzilli C.E.N., Simple formulas for the natural frequencies of non-uniform cables and beams. Int. J. Mechanical Sciences 77 (2013) 155–163. https://doi.org/10.1016/j.ijmecsci.2013.09.028

[2] Sachdev P.L., Self-similarity and beyond. Exact solutions of nonlinear problems, 2020. Chapman and Hall. ISBN: 9780367455484

[3] Harvey T.J., Alto P., Natural forcing functions in non-linear systems. J. Applied Mechanics 25 (1958) 352-356.

[4] Hsu C.S., On the application of elliptic functions in nonlinear forced oscillations. Quaterly of Applied Mathematics 17 (1960) 393-407.

[5] Duffing G., Erzwungene Schwingungen bei veränderlicher Eigenfrequenz und ihre technische bedeutung (Forced oscillators with variable eigenfrequency and their technical meaning), Vieweg & Sohn, Sammlung Vieweg, 1918, pp. 41–42 (In German).

[6] Byrd P.F. , Friedman M.D., Handbook of Elliptic Integrals for Engineers and Scientists, 1971. Berlin, Heidelberg, New York. ISBN 978-3-540-05318-7

[7] Rakaric Z., Kovacic I., Cartmell M., On the design of external excitations in order to make nonlinear oscillators respond as free oscillator of the same or different type. Int. J. Non-Linear Mechanics 94 (2017) 323-333. https://doi.org/10.1016/j.ijnonlinmec.2016.06.012

[8] Vakakis A.F., Blanchard A., Exact steady states of the periodically forced and damped Duffing oscillator. J. Sound and Vibration 413 (2018) 57-65. https://doi.org/10.1016/j.jsv.2017.10.030

[9] Kovacic I., Externally excited undamped and damped linear and nonlinear oscillators: Exact solutions and tuning to a desired exact form of the response. Int. J. Non-Linear Mechanics 102 (2018) 72-81. https://doi.org/10.1016/j.ijnonlinmec.2018.03.010

[10] Caughey T.K., Vakakis A.F., A method for examining steady state solutions of forced discrete systems with strong non-linearities, Int. J. Non-Linear Mechanics 26 (1991) 89-103. https://doi.org/10.1016/0020-7462(91)90083-6

[11] Kovacic I., Zukovic M., Coupled purely nonlinear oscillators: normal modes and exact solutions for free and forced responses. Nonlinear Dynamics 87 (2017) 713-726. https://doi.org/10.1007/s11071-016-3070-0

[12] Kovacic I., Zukovic M., On the response of some discrete and continuous oscillatory systems with pure cubic nonlinearity: Exact solutions. Int. J. Non-Linear Mechanics 98 (2018) 13-22. https://doi.org/10.1016/j.ijnonlinmec.2017.09.009

[13] Kerschen G., Peeters M., Golinval J.C., Vakakis A.F., Nonlinear normal modes, Part I: A useful framework for the structural dynamicist. Mechanical Systems and Signal Processing 23 (2009) 170-194. https://doi.org/10.1016/j.ymssp.2008.04.002

[14] Peeters M., Viguié R., Sérandour G., Kerschen G., Golinval J.C., Nonlinear normal modes, Part II: Toward a practical computation using numerical continuation techniques. Mechanical Systems and Signal Processing 23 (2009) 195-216. https://doi.org/10.1016/j.ymssp.2008.04.003

[15] Xu Y., Luo A.C.J., Series of Symmetric Period-1 Motions to Chaos in a two-degree-of-freedom van der Pol-Duffing Oscillator. Journal of Vibration Testing and System Dynamics 2(2) (2018) 119-153. https://doi.org/10.5890/JVTSD.2018.06.003

[16] Musielak D.E., Musielak Z.E., Benner J.W., Chaos and routes to chaos in coupled Duffing oscillators with multiple degrees of freedom. Chaos, Solitons and Fractals 24 (2005) 907–922. https://doi.org/10.1016/j.chaos.2004.09.119

[17] Vincent U.E., Njah A.N., Akinlade O., Solarin A.R.T., Synchronization of cross-well chaos in coupled Duffing oscillators. Int. J. Modern Physics B 19 (2005) 3205–3216. https://doi.org/10.1142/S0217979205032085

[18] Sabarathinam S., K. Thamilmaran K., Borkowski L., Perlikowski P., Brzeski P., Stefanski A., Kapitaniak T., Transient chaos in two coupled, dissipatively perturbed Hamiltonian Duffing oscillators. Communications in Nonlinear Science and Numerical Simulation 18 (2013) 3098-3107. http://dx.doi.org/10.1016/j.cnsns.2013.04.002

[19] Jothimurugan R., Thamilmaran K., Rajasekar S., Sanjuán M.A.F., Multiple resonance and anti-resonance in coupled Duffing oscillators. Nonlinear Dynamics 83 (2016) 1803–1814. https://doi.org/10.1007/s11071-015-2447-9

[20] Clementi F., Lenci S., Rega G., 1:1 internal resonance in a two d.o.f. complete system: a comprehensive analysis and its possible exploitation for design. Meccanica 55 (2020) 1309-1332. https://doi.org/10.1007/s11012-020-01171-9

[21] Haddow A.G., Barr D.S., Mook D.T., Theoretical and experimental study of modal interaction in a two-degree-of-freedom structure. J. Sound Vibr. 97 (1984) 451-473. https://doi.org/10.1016/0022-460X(84)90272-4

[22] Kyzioł J., Okniński A., Metamorphoses of resonance curves in systems of coupled oscillators: The case of degenerate singular points. Int. J. Non-Linear Mechanics 95 (2017) 272–276. https://doi.org/10.1016/j.ijnonlinmec.2017.07.004

[23] Kyzioł J., Okniński A., Effective equation for two coupled oscillators: Towards a global view of metamorphoses of the amplitude profiles. Int. J. Non-Linear Mechanics 123 (2020) 103495. https://doi.org/10.1016/j.ijnonlinmec.2020.103495

[24] Guin A., Dandapathak M., Sarkar S., Sarkar B.C., Birth of oscillation in coupled non-oscillatory Rayleigh–Duffing oscillators. Communications in Nonlinear Science and Numerical Simulation 42 (2017) 420–436. http://dx.doi.org/10.1016/j.cnsns.2016.06.002

[25] Hill T.L., Cammarano A. Neild S.A., Wagg D.J., Interpreting the forced responses of a two-degree-of-freedom nonlinear oscillator using backbone curves. J. Sound Vibr. 349 (2015) 276-288. http://dx.doi.org/10.1016/j.jsv.2015.03.030

[26] Abramowitz M., Stegun I.A. (Eds.), Handbook of mathematical functions, 9^{th} edition, 1970. Dover Publications, New York. ISBN 486-61272-4

[27] Raj S.P., Rajasekar S., Murali K., Coexisting chaotic attractors, their basin of attractions and synchronization of chaos in two coupled Duffing oscillators. Physics Letters A 264 (1999) 283-288. https://doi.org/10.1016/S0375-9601(99)00817-8

[28] Andonovski N., Lenci S., Six-dimensional basins of attraction computation on small clusters with semi-parallelized SCM method. Int. J. Dynamics and Control 8 (2020) 436–447. https://doi.org/10.1007/s40435-019-00557-2

[29] Lenci S., Clementi F., Kloda L., Warminski J, Rega G., Longitudinal-transversal internal resonances in Timoshenko beams with an axial elastic boundary condition. Nonlinear Dynamics 103 (2021) 3489-3513. https://doi.org/10.1007/s11071-020-05912-z

[30] Xia C., Wang D.F., Ono T., Itoh T., Esashi M., Internal resonance in coupled oscillators - Part I: A double amplification mass sensing scheme without Duffing nonlinearity. Mechanical Systems and Signal Processing 159 (2021) 107886. https://doi.org/10.1016/j.ymssp.2021.107886

[31] Xia C., Wang D.F., Ono T., Itoh T., Esashi M., Internal resonance in coupled oscillators – Part II: A synchronous sensing scheme for both mass perturbation and driving force with Duffing nonlinearity. Mechanical Systems and Signal Processing 160 (2021) 107887. https://doi.org/10.1016/j.ymssp.2021.107887

[32] Noël J.P., Detroux T., Masset L., Kerschen G., Virgin L. N., Isolated Response Curves in a Base-Excited, Two-Degree-of-Freedom, Nonlinear System. in Proc. of ASME-IDETC Conference, paper No: DETC2015-46106, V006T10A043. https://doi.org/10.1115/DETC2015-46106

[33] Gatti G., Brennan M.J., Inner detached frequency response curves: an experimental study. J. Sound and Vibration 396 (2017) 246-254. http://dx.doi.org/10.1016/j.jsv.2017.02.008

[34] Kuether R.J., Renson L., Detroux T., Grappasonni C., Kerschen G., Allen M.S., Nonlinear normal modes, modal interactions and isolated resonance curves. J. Sound and Vibration 351 (2015) 299-310. http://dx.doi.org/10.1016/j.jsv.2015.04.035